

THE ORIGIN OF THE X-RAY AND ULTRAVIOLET EMISSION IN NGC 7469

K. Nandra^{1,2}, T. Le^{2,3}, I.M. George^{1,2}, R.A. Edelson^{4,5}, R.F. Mushotzky¹, B.M. Peterson⁶,
T.J. Turner^{1,7}

ABSTRACT

We present a spectral analysis of a ~ 30 d, near-continuous observation of the Seyfert 1 galaxy NGC 7469 with *RXTE*. Daily integrations show strong spectral changes during the observation. Our main result is that we find the X-ray spectral index to be correlated with the UV flux. Furthermore, the *broad-band* X-ray photon flux is also correlated with the UV continuum. These correlations point towards a model in which the X-rays originate via thermal Comptonization of UV seed photons. Furthermore, the UV is also correlated with the extrapolation of the X-ray power law into the soft X-ray/EUV region. Our data analysis therefore re-opens the possibility the the UV photons and their variability arise from reprocessing, as long as the primary source of heating is photo-electric absorption in the reprocessor, rather than Compton downscattering. A coherent picture of the X-ray/UV variability can therefore be constructed whereby absorption and reprocessing of EUV/soft X-rays in a standard accretion disk produce a variable seed photon distribution which are in turn up-scattered into the X-ray band. We also find a significant correlation between the 2-10 keV flux and the 6.4 keV iron $K\alpha$ line suggesting that at least some portion of the line originates within ~ 1 lt day of the X-ray continuum source. Neither the power law photon index nor the Compton reflection component are correlated with the 2-10 keV flux. The latter is not correlated

¹Laboratory for High Energy Astrophysics, Code 660, NASA/Goddard Space Flight Center, Greenbelt, MD 20771

²Universities Space Research Association

³Department of Physics and Astronomy, George Mason University, Fairfax, VA 22030

⁴Department of Astronomy, University of California, Los Angeles, CA 900024

⁵X-ray Astronomy Group, Leicester University, Leicester LE1 7RH, UK

⁶Department of Astronomy, Ohio State University, 174 West 18th Avenue, Columbus, OH 43210

⁷University of Maryland, Baltimore County, 1000 Hilltop Circle, Baltimore, MD 21250

with the iron $K\alpha$ line flux either. We do find an apparent correlation between the X-ray spectral index and the strength of the Compton reflection component. In an Appendix we show, however, that this can be produced by a combination of statistical and systematic errors. We conclude the apparent variations in the Compton reflection component may be an artifact of these effects.

Subject headings: galaxies:active – galaxies: nuclei – galaxies: individual (NGC 7469) – ultraviolet: galaxies – X-rays: galaxies

1. INTRODUCTION

Active galactic nuclei (AGN) emit most of their bolometric luminosity in the “big blue bump” (BBB), which dominates the optical, ultraviolet (UV) and Extreme Ultraviolet (EUV) emission, unless the regions which produce these components are obscured. A further ubiquitous property of AGN is hard X-ray emission, which is spectrally distinct from the big blue bump and energetically significant. With the exception of strong radio emission, which is only observed in a small fraction of AGN, all other components of the AGN spectrum can typically be accounted for by some kind of “reprocessing”, by which we mean passive absorption and re-radiation, without significant additional energy input. Thus the BBB and X-ray continua can be considered the “primary” emissions of AGN and determining their origin holds the key to our understanding of the central engine of active galaxies.

The evidence for black holes in AGN is now extremely strong (e.g. Miyoshi et al. 1995; Tanaka et al. 1995) but the fueling and emission mechanism are still not well known. The probable presence of angular momentum lead naturally to the hypothesis of an optically-thick accretion disk around the black hole (e.g. Lynden-Bell 1969) which radiates the BBB (Shields 1979; Malkan & Sargent 1982). A disk geometry can also account for some optical line profiles (e.g. Chen, Halpern & Filippenko 1989; Eracleous & Halpern 1994) and explain the profiles of the broad, redshifted iron lines (e.g., Fabian et al. 1995; Nandra et al. 1997). Accretion disk models are not free from problems, however. A significant difficulty is the presence of extremely rapid, wavelength independent variations in flux (e.g. Clavel et al. 1991; Peterson et al. 1991). Standard disks should show time lags between optical and UV bands as instabilities propagate through them, but these lags should be much longer than the observed upper limits (e.g. Courvoisier & Clavel 1991; Krolik et al. 1991; Molendi, Maraschi & Stella 1992).

X-ray illumination of the disk may offer a way of explaining these rapid, wavelength-independent variations of the optical/UV continuum. Guilbert & Rees (1988) were first to suggest that dense, optically thick material could reprocess and thermalize the X-ray emission of AGN, re-emitting the radiation in the BBB. If that material were the accretion disk, variations in the reprocessed flux could occur on the order of the light-travel time, which is compatible with the observations. An apparent time lag of ~ 1 d between the short-wavelength UV and optical variations in NGC 7469 (Wanders et al. 1997; Collier et al. 1998; Peterson et al. 1998; Kriss et al. 2000) offers further support for this hypothesis. X-ray fluorescence and Compton scattering in the disk then account for the iron lines and hard tails observed in the X-ray spectra (Nandra & Pounds 1994).

The illuminating hard X-ray emission is a separate component not predicted by standard disk models and requires another emission mechanism. Currently-popular thinking is that the X-rays arise from a “corona” which Compton up-scatters softer “seed” photons (e.g. Sunyaev & Titarchuk 1980), presumably from the optical/UV where there is an abundant photon field. Such models reproduce the broadband characteristics of the X-ray spectrum (e.g. Haardt & Maraschi 1991, 1993), especially if the corona is patchy (Stern et al. 1995). A patchy, flaring corona is also suggested by the variability of the iron $K\alpha$ lines (Iwasawa et al. 1996, 1999; Nandra et al. 1999). A high energy cutoff at ~ 200 keV observed in some sources argues for a thermal distribution of upscattering particles (Zdziarski et al. 1994; Gondek et al. 1996).

A reasonably coherent picture of the central regions of AGN can thus be constructed where an accretion disk surrounds a supermassive black hole, with active flaring regions above the disk. The BBB photons produced from the thermal emission of the disk are Compton-up-scattered in the flaring regions, producing the X-ray continuum. This continuum then illuminates the disk, producing more (and rapidly variable) optical/UV emission via reprocessing, the iron line via fluorescence, and the reflection hump from Compton downscattering.

In the simplest such picture, the UV and X-ray variations should be strongly correlated as they are tied together by two mechanisms, the upscattering of the UV photons producing the X-rays, and the reprocessing of the X-rays into UV. Any time lags between the two bands should be very small, being just the light travel time between the regions, and their sense would indicate which of the two mechanisms were the dominant one. Some early observations did indeed suggest a link between the UV and X-ray bands (Clavel et al. 1992; Edelson et al. 1996) and between the UV and EUV (Marshall et al. 1997) consistent with reprocessing. More recent observations have shown a relationship between the EUV and X-rays, supporting Comptonization (Chiang et al. 2000; Uttley et al. 2000). Nandra et

al. (1998; hereafter N98), however, have presented a ~ 1 month, near-continuous *RXTE* monitoring campaign on NGC 7469, with simultaneous UV data from IUE (Wanders et al. 1997). N98 found a poor correlation between the 2-10 keV X-rays and short wavelength (1315 Å) UV at zero lag, with strong X-ray variations on short timescales but none in the UV. The maxima in the UV emission appeared to lag the X-ray peaks by about 4d, but the minima were near-simultaneous. These effects are difficult to explain in the context of the relatively-simple and observationally attractive picture of the central engine outlined above.

The NGC 7469 observations have apparently left both reprocessing and Comptonization models at a dead end, at least for that source. Similar behavior has been observed in NGC 3516, with a poor zero-lag correlation between the 2-10 keV X-rays and the optical flux observed both on short (\sim day) and long (\sim month) time scales (Edelson et al. 2000; Maoz, Edelson & Nandra 2000). This invites extrapolation to AGN as a class, and leaves contradictory and conflicting evidence as to the existence of the accretion disk, the importance of reprocessing and the origin of the X-rays. Here we present a spectral analysis of the *RXTE* data for NGC 7469 which, when compared to the X-ray and UV continuum data, appears to resolve these conflicts and contradictions. After describing the observations and analysis technique briefly in Section 2, we discuss the *RXTE* spectral properties of NGC 7469 in Section 3. In Section 4 we discuss time variability of the spectrum and the correlations between the X-ray spectral properties and in Section 5 discussion the correlations of those properties with the UV. In section 6 we discuss the results.

2. OBSERVATIONS

Many of the details of the *RXTE* observations are described in N98. The primary difference between their data reduction and ours is in the employment of the new background model, known as the “L7+activation” model. This provides a reduction in the systematic errors, allowing spectral analysis. We applied the standard selection criteria in the “rex” *RXTE* processing script. These excluded periods where the earth elevation angle was less than 10 degree, where the offset between the pointing position and the source was greater than 0.02 degree, a 30 minute period after passage through the SAA and times where anomalous electron flares occurred. We restricted our analysis to the three PCU’s which were operating throughout the observation for reasons of uniformity and simplicity.

Even with the new model, the background-subtraction is unreliable at high energies for relatively weak sources such as NGC 7469. We have therefore restricted our analysis to the 2-20 keV band, and consider the possibility of systematic errors in subtraction in our analysis. We calculated response matrices using PCARSP v2.37. We calculated matrices

for several different times of the observation, but found no statistically significant difference between the derived spectra. We have therefore employed a single matrix for the entire observation, calculated for a spectrum in the middle of the observational period.

The standard software estimates the error in the net (source minus background) rate by combining the errors in the total rate with those of the simulated background. The background estimation software calculates errors on the simulated background spectrum assuming Poisson statistics appropriate for the period simulated. In practice this is a considerable overestimate of the statistical error on the background spectrum, which is estimated using a large amount of data. Indeed, the statistical error in the background estimation should typically be negligible compared to the error on the total rate. We have therefore assumed zero error on the estimated background, and calculate the error in the background-subtracted count rate based only on the error in total rate. This is obviously not strictly correct and will result in an underestimate of the statistical errors which may become apparent in a very long integration. More importantly, it also ignores any systematic error. Later, we discuss in detail whether systematic errors in the background subtraction are likely to affect our results.

In many cases below we have estimated X-ray power-law fluxes in bands either broader than or far removed from the observed *RXTE* (2-20 keV) band. In such cases the error on the flux is dominated by the uncertainty in the extrapolated spectral model. In order to determine the flux values and uncertainties we have therefore searched through the parameter space defined by the 68 per cent confidence contours for the spectral parameters, determining the minimum and maximum fluxes consistent with the data at this confidence level. From these we adopt the mean of the maximum and minimum values as our flux estimate, and the error to be half the difference between the maximum and minimum.

The IUE observations used here are described in Wanders et al. (1997) and we have used the modified light curve derived by Kriss et al. (2000) for all plots and correlations, which improves over the original Wanders et al. light curve by taking account of low contrast line features. In calculating UV fluxes for comparison with derived X-ray spectral properties, we have taken an average of the (typically 3-5) IUE spectra taken during the X-ray integrations. For the error bar on the UV points, we adopt the larger of the dispersion of the individual IUE points, and the propagated Kriss et al. errors.

3. Integrated X-ray spectrum

The *Ginga* data first showed the presence of an iron $K\alpha$ line and reflection hump in NGC 7469 (Piro et al. 1990; Nandra & Pounds 1994). *ASCA* confirmed the presence of the line, but a controversy remains as to whether the line is broad or not, with Guainazzi et al. (1994) finding no evidence for significant width and Nandra et al. (1997) finding marginal evidence. This issue is largely irrelevant for *RXTE*, however, which has much poorer spectral response than the *ASCA* SIS. We therefore fitted the spectrum of NGC 7469, integrated over the entire 30 day period, with a model consisting of a power law, a gaussian to represent the iron $K\alpha$ line and a reflection component (pexrav; Magdziarz & Zdziarski 1995). In the reflection model, we assume no high-energy cutoff in the incident power law, and that the reflection is from an optically thick slab inclined to our line of sight with an inclination, i , corresponding to $\cos i = 0.95$, the lowest inclination allowed in the model.

The spectral fits to a simple power law and this more complex model are shown in Fig. 1. In these fits we fixed the absorption column at the Galactic value, derived from 21 cm measurements of 4.9×10^{20} cm (Elvis, Lockman & Wilkes 1989). The *RXTE* data are insensitive to column densities $< \text{few} \times 10^{21}$ cm $^{-2}$, for which there is no evidence from the *ASCA* or *ROSAT* spectra, which extend to lower energies (Brandt et al. 1993; Guainazzi et al. 1994). Although we did find a formal improvement when the column was allowed to be free ($\Delta\chi^2=30$), this is due to a very small deviation (~ 2 per cent) in the very lowest energy bin. We therefore consider the apparent absorption to be due to small systematic effects in the calibration and/or background subtraction.

In contrast the iron line and reflection hump represent much larger deviations, both in percentage and χ^2 senses. The inclusion of the iron line reduces χ^2 by 1600 compared to a power law, and the Compton reflection further reduces it by $\Delta\chi^2=330$. These are obviously highly significant reductions in a statistical sense. The deviations due to the iron line and reflection hump are of order 10 per cent (Fig. 1). The fit is not formally acceptable with $\chi^2=144.7/41$ d.o.f., which is rejected at very high confidence. The residuals below about 15 keV are < 3 per cent, however, and could be due to the above-mentioned systematic errors. Another possible reason for the poor fit is that, as we show below, NGC 7469 undergoes substantial spectral variation during the observation. The combination of several, dissimilar spectra would result in integrated data which were difficult to fit. We have not therefore sought a more complex model, and adopt the power law, gaussian and reflection fit as our test model in investigating the spectral variability below. The parameters from the integrated fit were a spectral index $\Gamma = 1.92 \pm 0.02$, line energy $E_{K\alpha} = 6.42 \pm 0.03$ keV and line flux $F_{K\alpha} = 5.1 \pm 0.3 \times 10^{-5}$ ph cm $^{-2}$ s $^{-1}$, corresponding to an equivalent width, EW =

150 ± 10 eV. The line equivalent width is consistent with that seen by *ASCA* (Guainazzi et al. 1994; Nandra et al. 1997). The mean 2-10 keV flux of $F_{2-10} = 3.28 \times 10^{-11}$ erg cm $^{-2}$ s $^{-1}$ corresponds to a 2-10 keV luminosity of 4.1×10^{43} erg s $^{-1}$.

The reflection normalization at 1 keV is $A_{ref} = 5.1_{-0.8}^{+1.0} \times 10^{-3}$ ph cm $^{-2}$ s $^{-1}$ keV $^{-1}$. The value of A_{ref} corresponds to the normalization of the illuminating power law, assuming 2π coverage. We define the reflection fraction R to be the ratio of A_{ref} to the observed normalization of the power law. In other words, R is the ratio of the strength of the reflection component to that expected from a face-on slab subtending 2π solid angle. For our data we find $R = 0.48_{-0.08}^{+0.09}$. On the face of it, this suggests that the solid angle subtended by the reflector is closer to π . There are, however, numerous reasons why the reflection fraction R might be lower than unity. First, the inclination might be higher than assumed (a face-on disk maximizes the reflection component), with projection effects reducing the strength of the reflection. If the assumed solid angle, spectral shape, and power law illumination are correct, we can therefore derive an inclination of $\cos i = 0.32_{-0.06}^{+0.07}$, corresponding to $i = 71^\circ \pm 4$.

Another possibility is that there is a cutoff in the primary spectrum, which reduces the number of high energy photons able to be down-scattered into the reflection hump. In this case we constrain the cutoff energy $E_c = 53_{-7}^{+10}$ keV, lower than is typical for Seyfert galaxies (Madejski et al. 1995; Gondek et al. 1996), but similar to, e.g., NGC 4151 (Maisack et al. 1993; Zdziarski, Johnson & Magdziarz 1996). The introduction of an exponential cutoff into the spectrum provides a significantly better fit ($\Delta\chi^2=42$). Given the uncertainties in the background modeling at the highest energies we consider this to be inconclusive, particularly as the HEXTE spectrum of this source appears to show a significant detection up to ~ 70 keV (R. Rothschild, priv. comm.). BeppoSAX also found no evidence for such a cutoff, with a lower limit $E_c > 230$ keV (Matt 2000; De Rosa et al. 2000). A final possibility is that the X-ray power law is anisotropic (cf. Ghisellini et al. 1991), with the X-rays beamed such that a factor $\sim R$ less flux travels towards the disk than reaches the observer directly.

4. Time-resolved spectral analysis

The values derived from the integrated spectrum are largely consistent with those found in the *Ginga* observations of NGC 7469 (Piro et al. 1990) and are rather typical of Seyfert 1 galaxies as a whole (Nandra & Pounds 1994). The real interest in our observation lies in any variations. In the simplest reflection picture, we would expect the line flux $F_{K\alpha}$ and the reflection flux A_{ref} to be closely coupled to the continuum flux, and to each other.

To investigate this we have divided our observation into 30 segments of approximately one day duration. These segments have exposure times ranging from about 13 to 21 ks (Table 1) which are sufficient to detect and constrain both the reflected flux and iron line. We fitted each of these spectra with a model consisting of a power law without high energy cutoff, a gaussian with energy fixed at the value for neutral iron of 6.4 keV and reflection component with free normalization A_{ref} . The results are shown in Table 1.

4.1. Light Curves

The light curves of F_{2-10} , Γ , $F_{K\alpha}$ and A_{ref} are shown in Figure 2. The bottom three panels show the UV continuum light curve at 1315Å, which we designate F_{UV} , and two other derived parameters which we discuss below. The top panel shows that F_{2-10} varies by ~ 50 per cent during the observation (N98). The photon index, Γ is also clearly variable, with $\chi^2=58.6/29$ d.o.f against a constant hypothesis (significant at > 99.9 per cent confidence), but is not simply related to the flux (see below). The iron line flux is consistent with a constant ($\chi^2=13.4/29$ d.o.f), but the best fit values show trends similar to that of the continuum flux. The reflection flux is again formally consistent with a constant ($\chi^2=21.0/29$ d.o.f), but appears to show trends similar to that of Γ .

A more sensitive way of detecting variations in the parameters is to use the F-test. We have repeated the fits to the daily spectra, but this time fixing each of the parameters (Γ , $F_{K\alpha}$, A_{ref}) at their mean values (1.91, 5.1×10^{-5} , 5×10^{-3}). We then compute the F-statistic by comparing the total χ^2 of these fits to the χ^2 when all parameters were free. We derived F values of 5.38, 1.28 and 2.08 for 30 additional parameters, implying highly significant changes in Γ and A_{ref} (> 99 per cent confidence) but only marginal changes in $F_{K\alpha}$. Nonetheless, we do believe there are variations in $F_{K\alpha}$ based on its correlation with the continuum. We now explore the correlations between these X-ray parameters.

4.2. X-ray/X-ray Correlations

The results of linear (Pearson) and rank (Spearman) correlations between the various X-ray parameters, assuming no time lags, are given in Table 2. The parameters are plotted against each other in Fig. 3. Two positive correlations have apparent significances of > 99 per cent confidence, F_{2-10} vs. $F_{K\alpha}$ and Γ vs. A_{ref} . A marginal (~ 95 per cent) anti-correlation is seen between A_{ref} and $F_{K\alpha}$.

As discussed by Welsh (1999) and Maoz et al. (2000), cross-correlation of light curves

which have a “red noise” character can result in spuriously high values of the correlation coefficient due to the fact that adjacent points in the light curve are highly correlated. This could cause us to overestimate the significance of the correlations we observe, due to the fact the the effective number of independent data points in the correlation is less than the actual number of data points. We have tested this in the case of the F_{2-10} vs. $F_{K\alpha}$ correlation by simulating a number of light curves with “red noise” power spectra (i.e. where the variability power scales as $f^{-\alpha}$, where f is the frequency). We adopt a value for the power law index of $\alpha = 1.3$, the best-fit value for a fit to the 2-10 keV power-density spectrum presented by N98. As we have no a priori information regarding the statistical characteristics of the line light curve, we have correlated the simulated continuum light curves with the real light curve of $F_{K\alpha}$ (Fig. 2). In 140 trials of 30 points, in no case did we find either a Pearson or Spearman correlation coefficient as high as that observed with the real data. The maximum values obtained were $r=0.52$ (Pearson) and $r=0.51$ (Spearman) compared to the $r=0.54/0.52$ found. We therefore conclude that the correlation between F_{2-10} and $F_{K\alpha}$ is unlikely to arise by chance coincidence.

The correlation we observe between the line and continuum fluxes indicates that the line emission comes from very close to the central regions, consistent with current thinking about the line origin (e.g. Tanaka et al. 1995; Nandra et al. 1997). Ideally, we would use such data to perform “reverberation mapping” of the inner accretion disk, similar to that which has been performed in the optical/UV (e.g. Blandford & McKee, 1982; Peterson 1993). With our current sampling and data quality this is not possible, but as these are arguably the best data obtained thus far for such a purpose, we have calculated the interpolation cross correlation function (Gaskell & Peterson 1987; White & Peterson 1994) between the line and continuum (Fig 6). The data are not of sufficient quality to place limits on the lag using the methods of, e.g. Peterson et al. (1998). Nonetheless, the fact that a significant correlation is observed is indicative that the line arises from within a few light days of the continuum source.

It is apparent from Fig. 2 that both Γ and A_{ref} are uncorrelated with the 2-10 keV continuum flux, confirmed by Fig. 3. Earlier observations, mostly with poorer data quality and sampling, had shown a tendency for a correlation between Γ and the X-ray flux (e.g. Turner 1987; Matsuoka et al. 1990; Leighly et al. 1996). As we shall show below, our data show that the situation may be more complex than a simple correlation between Γ and X-ray flux. Indeed the Γ light curve of NGC 7469 is reminiscent of the *ultraviolet* emission of NGC 7469 which we also plot in the Fig. 2, along with two other quantities derived from the X-ray spectra. We explore these further below.

The lack of correlation between A_{ref} and the F_{2-10} , or A_{ref} and $F_{K\alpha}$ is difficult to

explain in the standard picture in which both arise from the same, small region (e.g. George & Fabian 1991; Matt, Perola & Piro 1991). We have reason, however, to believe that the derived values of A_{ref} may not be truly representative of the strength of the reflection component.

A high correlation coefficient is obtained for Γ vs. A_{ref} (Table 1; see also Zdziarski, Lubinski & Smith 1999), but great caution must be exercised when attempting to correlate spectral parameters which were derived from a single fit with a low spectral resolution detector. This is because the parameters are often correlated in the fit, and thus a particular value of one might lead statistically and systematically to a certain value of another (see also Matt 2000). We discuss this further in Appendix A, where we have performed simulations which show that a combination of statistical and systematic errors can account for the observed correlation. We therefore assign no statistical confidence to the Γ/A_{ref} correlation and make no explicit interpretation of it. We further assign no significance to the lack of correlations between A_{ref} and F_{2-10} or $F_{K\alpha}$.

5. X-ray/UV correlations

Fig. 5 shows a number of X-ray spectral parameters and fluxes plotted against the UV continuum flux (Wanders et al. 1997; Kriss et al. 2000). Correlation coefficients are shown in Table 2. There is a clear correlation between F_{UV} and the X-ray spectral index Γ . We also find a marginal correlation between the UV continuum and reflection component, A_{ref} , but this is most likely to be an artifact of the (real) correlation between Γ and F_{UV} , combined with the (possibly spurious) correlation between Γ and A_{ref} (see Appendix A). We have again performed simulations to test whether the $F_{\text{UV}}-\Gamma$ correlation is due to chance coincidence when dealing with red noise light curves. This time we adopt an index $\alpha = 1.9$ for the simulated light curves (the best-fit value for the F_{UV} PDS of N98) and correlated them with the real Γ light curve. Once again, with 140 trials, we failed to find a correlation coefficient as significant as that which we obtained. Here we found maximum values of 0.69/0.69 (linear/rank) compared to 0.81/0.89 observed.

We now consider some possible interpretations of the Γ/F_{UV} correlation. The first is that the UV flux is simply an extrapolation of the X-ray power law to 1315Å. We have tested this by performing such an extrapolation, and the derived values F_{UVextrap} are plotted in Fig. 2 and against F_{UV} in Fig. 5. We indeed see a correlation between the two, but F_{UVextrap} is a factor ~ 3 less than the observed flux. One explanation for this is that the extrapolated (and variable) X-ray component lies on top of a stronger uncorrelated component (perhaps the disk flux), in this case having a flux of $\sim 3 \times 10^{-15}$ erg cm $^{-2}$ Å $^{-1}$.

The addition of such a component to the extrapolated X-ray flux almost reproduces the observed UV light curve, but the amplitude of variation of the real light curve is greater than the extrapolated one. Furthermore, in the general case (though not necessarily in NGC 7469), the UV shows a flatter spectral slope than the X-rays. We conclude that a simple extrapolation of the X-ray spectrum is unlikely to be the origin of the UV flux.

Nonetheless we note with great interest that if the soft X-ray/EUV flux of NGC 7469 is a simple extrapolation of the harder X-ray power law we measure with *RXTE*, the soft X-rays and UV would be highly correlated. Such a correlation could revive reprocessing models for the UV, as long as the reprocessing was primarily of soft X-rays. The best way of establishing the connection between the soft X-ray and UV is of course to correlate them directly. Our *RXTE* data have a lower threshold of ~ 2 keV and are therefore not ideal for this purpose. We have, however, attempted this in a comparative way by correlating the *RXTE* 2-4 keV and 7-12 keV fluxes (which have similar signal-to-noise ratios) with F_{UV} . We did find a higher correlation coefficient ($r = 0.34$ for a Pearson correlation) for the soft X-rays than for the hard ($r = 0.07$). The soft X-ray correlation is not significant, however, making it difficult to draw firm conclusions from this analysis. Our conclusion of a soft X-ray/UV correlation therefore relies on the model-dependent assumption that the hard X-ray power law extrapolates to lower energies. While we note that, if there are additional soft X-ray emission components, this may not be valid the *ASCA* and *ROSAT* data both indicate that a single component dominates the emission over the whole X-ray band. We therefore offer below an interpretation of the correlation between the extrapolated soft X-ray flux and F_{UV} .

Another reason why the UV flux and X-ray spectral index could be related is if the X-rays arise from Comptonization of the UV photons in a corona. When the UV flux increases, this should cool the corona resulting in a softer Comptonized spectrum. This was one of the possibilities that the UV/X-ray variability campaign was designed to test, and in such a scenario we expect a correlation between the X-ray and UV fluxes. In the presence of spectral variability, however, as we observe here, it is not clear whether a given narrow-band (e.g. 2-10 keV) flux should show the correlation. In the Comptonization process energy is added to the seed photons by the corona, which eventually emerge at some X-ray energy. For a cool corona, more photons would emerge at low energies, while a hotter one would have relatively more hard X-ray photons. Regardless of the properties of the corona, however, we should expect each UV photon up-scattered to result in one emerging X-ray photon. We would therefore expect a correlation between the UV flux and the broad band X-ray photon flux. We plot the 0.1-100 keV photon flux, $Q_{0.1-100}$ in Figs 2 and 5 also. It can be seen that this is also correlated with the UV flux (and also with Γ and $F_{UV\text{extrap}}$), and this again supports the Comptonization model.

Confirming the results of N98, we find no significant correlation between F_{2-10} and F_{UV} . We neither find any relationship between F_{UV} and $F_{K\alpha}$.

6. DISCUSSION

Spectral analysis of the *RXTE* data during the 30 day simultaneous campaign with IUE has revealed further important information regarding the X-ray and UV emission in AGN. A significant correlation is observed between the 2-10 keV X-ray flux and the flux of the iron $K\alpha$ line. The other significant correlation observed within the X-rays is between Γ and the strength of the reflection component, similar to that seen by Zdziarski et al. (1999) when comparing the properties of a heterogeneous sample of AGN. In our *RXTE* data, such a correlation can be produced spuriously, however, by a combination of statistical and systematic effects, and we assign no confidence to it or the (most likely secondary) correlation between A_{ref} and the UV flux (Appendix A). We do find a significant correlation between the X-ray spectral index and the UV flux of NGC 7469. We also find that the broad-band X-ray photon flux is well correlated with the UV, as is the X-ray power law flux extrapolated back into the EUV/soft X-ray band. We now discuss these results and what they tell us about the nature of the emission mechanisms and reprocessing region in NGC 7469.

6.1. Origin of the X-ray continuum

Our data strongly support the idea that the X-rays in NGC 7469 are produced by Compton upscattering of UV photons. We account for the changing spectral slope by hypothesizing that an increase in the UV seed photons cools the Comptonizing corona and producing a soft X-ray power law slope (e.g. Haardt, Maraschi & Ghisellini 1994; Zdziarski et al. 1999). We also observed a correlation between the broad-band X-ray photon flux and the observed UV flux. This is also expected in Comptonization models, where an increase in the UV photon field should provide a corresponding increase in the number of X-ray photons which eventually emerge from the corona. The behavior of NGC 7469 in this respect is similar to that observed in the state changes of galactic black-hole candidates (GBHC; e.g. Ebisawa, Titarchuk & Chakrabati 1996; Gierlinski et al. 1999), which show a steeper hard X-ray slope in the “high” state, where the soft X-ray flux is dominant.

6.2. Origin of the UV continuum

As we have mentioned above, a possible connection could exist between the X-ray and UV fluxes if the latter is simply an extrapolation of the X-ray spectrum. This might be the case if a broadband continuum were generated by synchrotron or synchrotron-self-Compton emission, as is thought to be the case in blazars. Such a model has an immediate attraction, as it can explain rapid, wavelength-independent variations in the UV without the problems associated with an accretion disk. In its simplest form, we can rule out this model as the extrapolated X-ray spectrum under-predicts the UV flux by a large factor. A further refinement of this idea is to introduce an additional, near-constant component to the UV. This could arise, for example, from the accretion disk and when added to the extrapolated flux could account for the emission. We again find this unlikely as then the amplitude of variability of the extrapolated flux is less than that observed. A further difficulty for this model is that the 2-10 keV X-rays show very rapid variations which are not observed in the UV (N98; see also Welsh et al. 1998). This is hard to account for if they both represent the same component.

Indeed, our data strongly suggest that the UV emission - or at least the variable part of the UV - arises from reprocessing of soft X-ray and/or EUV photons. N98 had concluded that reprocessing was unlikely, based on the fact that F_{2-10} and F_{UV} were poorly correlated at zero lag. Reprocessing models do indeed predict a correlation between the X-rays and UV but our spectral data have shown that the lack of a correlation in the case of NGC 7469 may have been due to the fact that we were observing a variable X-ray spectrum over a limited bandpass. In the Compton reflection/reprocessing scenario, two mechanisms can heat the reprocessing medium: absorption of soft X-rays, or Compton scattering of hard X-rays. The assumption of N98 was that the 2-10 keV X-ray flux was a good measure of these mechanisms. The spectral data have shown that this is not necessarily the case and, in particular, if the heating of the reprocessor is dominated by absorption of soft X-ray and EUV photons, we find our data to be entirely consistent with the reprocessing scenario. Soft X-ray absorption is a more efficient heating process than Compton scattering, as the cross sections are large below ~ 10 keV, and the photons deposit all of their energy when absorbed, compared to only a fraction $E/m_e c^2$ for scattering, where E is the photon energy.

Scattering can dominate the heating, however, in cases either where the reprocessor is highly ionized - reducing the absorption cross-section for soft X-rays - or if the intrinsic spectrum is very flat such that the hard X-rays are energetically dominant. In either scenario, even with a variable spectrum, one would expect the medium/hard X-rays (> 10 keV) to dominate the reprocessing. In NGC 7469 we see a range of spectral indices $\Gamma \sim 1.7 - 2.0$. Assuming an X-ray spectrum extending between 0.1 and 100 keV and a

near-neutral reprocessor, we would expect soft X-ray absorption to dominate in the soft state (i.e. when the UV flux is high) but to have more equal contributions in the harder state (i.e. where the UV flux is weak). For the soft state, which has $\Gamma = 2.0$, the 0.1-10 keV flux (which can be absorbed) is a factor ~ 2 greater than 10-100 keV flux (which is more likely to scatter). In the harder state, with $\Gamma = 1.7$, they are comparable. This accounts for the fact that N98 observed the minima in F_{2-10} and F_{UV} simultaneously, as at those times F_{2-10} is a good representation of the heating flux. At high UV fluxes (and therefore steep X-ray slopes), however, soft X-ray heating dominates, and F_{2-10} is not a good representation of the heating. This accounts for the lack of simultaneity between the maxima in F_{2-10} and F_{UV} noted by N98.

N98 estimated the luminosity available for reprocessing, showing that it was just sufficient to account for the UV flux at the shortest (observed) wavelength of 1315Å. The luminosity was not, however, sufficient to account for the whole of the optical/UV continuum. In practice, the reprocessing only needs to account (and in some geometries *should* only account) for the variable part of the optical/UV emissions. To estimate the luminosity of the variable component, we have created a “difference” spectrum of the variations by subtracting the approximate maximum and minimum fluxes of NGC 7469 in the optical/UV (Collier et al. 1998; Kriss et al. 2000). The observational data cover the wavelength range 1315Å-6850Å. We then fitted this difference spectrum with a power law, and integrated it from 912Å- 10,000Å, obtaining a peak-to-peak variable flux of 4.3×10^{-11} erg cm⁻² s⁻¹. The difference between the estimated X-ray fluxes in the 0.1-10 keV band at these times was 4.1×10^{-11} erg cm⁻² s⁻¹ (we crudely assume the X-rays above 10 keV are scattered, rather than absorbed). These are obviously comparable, although a fair comparison would require knowledge of the geometry and ionization of the reprocessor. We conclude, however, that soft X-ray reprocessing is an energetically plausible source of the variable UV emission.

6.3. Nature of the reprocessing regions

The observed correlation between F_{2-10} and $F_{K\alpha}$ does not suffer from the complexities mentioned above, as the 2-10 keV flux should closely follow the $\sim 7 - 10$ keV flux which excites the emission line. Although we established a significant correlation at zero lag, we were unable to set limits on the lag due to very low signal-to-noise ratio in the line. The observed correlation implies that at least some part of the line comes from very close to the central source. This supports current thinking that the line arises due to X-ray illumination of the inner accretion disk, based on the line profiles (e.g. Tanaka et al. 1995; Nandra et

al. 1997). There is no high signal-to-noise ratio profile of the iron $K\alpha$ line in NGC 7469, so there remains controversy as to whether it exhibits the characteristic, broad profile of an accretion disk. Our variability data are certainly consistent with there being a constant component to the line from material further away from the nucleus, such as the optical BLR (e.g. Holt et al. 1980) or the molecular torus envisaged in Seyfert 1/2 unification schemes (e.g. Ghisellini, Haardt & Matt 1993; Krolik, Madau & Zycki 1993).

Because of the potential systematic effects mentioned in appendix A, we can draw no conclusion about the origin or location of the reflection component. The two simplest cases have the reflection arising in the accretion disk, in which case it should be well correlated with the hard X-ray flux and the iron line, or the molecular torus, when it would remain roughly constant in strength and shape during the period of our observation. Neither is suggested by the data if taken at face value, but we await future data with better sensitivity and smaller systematic errors before drawing any conclusion.

If the variable UV emission does indeed arise from reprocessing of soft X-ray and EUV photons, as seems likely, we can make some inferences regarding the reprocessing region. The fact that no rapid variability is observed in the UV, while the X-rays show large-amplitude flares on short time scales (N98) indicates that the UV comes from a region more extended than the X-rays. Light-travel effects could then smear the fast variations. Berkley, Kazanas & Ozik (2000) have attempted to model the X-ray/UV variations of NGC 7469 taking into account the smearing by an accretion disk. They were unable to smooth out the fast X-ray variations in such a way as to reproduce the UV light curve. This may also provide difficulties for the soft X-ray-UV reprocessing model proposed here, although the Berkley et al. calculations would have to be repeated in the light of the spectral variations we observe here. It should also be noted that we have not actually observed rapid soft X-ray/EUV variations, merely inferred them from the presence of harder X-ray variability. If the rapid flares in the X-ray light curve seen by N98 had hard spectra (e.g. if they were absorbed), they might not have a measurable effect on the UV light curve.

It is apparent from the spectral energy distribution of N98 that the overall energetics of NGC 7469 cannot be dominated by reprocessed X-rays. In particular, the starburst and other galactic emission make a large contribution in the IR and optical (Genzel et al. 1995). It also seems likely that there is a relatively-steady contribution to the UV emission, perhaps intrinsic thermal emission from the accretion disk. These should also act as a seed source for the X-rays and one could envisage either UV emission mechanism being dominant at any given time in a single source, or when comparing different sources. It appears that in NGC 7469, at least at the epoch observed, the two mechanisms made rather similar contributions to the short-wavelength UV flux.

6.4. Origin of the variability

A significant problem for standard accretion disk models has been their inability to reproduce the observed rapid variations in the optical/UV, which show at most small time lags at different wavelengths (Clavel et al. 1991). This is not a problem for reprocessing models, as variations can occur as fast as the light travel time (e.g. Clavel et al. 1992). Our data show that reprocessing in a standard accretion disk can account for the observed UV variability data in NGC 7469, as long as the dominant heating process is absorption of soft X-rays. Thus variations in the soft X-ray flux could drive the UV variations.

As we now also have strong evidence, however, that the X-rays are produced by Compton upscattering of UV photons, the inverse could hold - in other words that UV variations drive those in the X-rays. Establishing which requires measurement of a time lag between the variations, which we have been unable to constrain. In practice, however, it seems likely that a “feedback” mechanism operates, with each band driving the other to some degree (Haardt & Maraschi 1993).

Such a “feedback” mechanism cannot obviously account for the rapid variations seen in F_{2-10} . Also, although we believe we have identified the radiation process which produces the X-rays (i.e. thermal Comptonization), the mechanism by which the X-ray corona is heated remains mysterious. Presumably that mechanism could induce intrinsic (and potentially rapid) X-ray variability, as noted by N98. There are very few specific models for heating the X-ray corona. Hot accretion disk/ADAF models (Shapiro, Lightman & Eardley 1976; Narayan & Yi 1994) heat the accreting gas to X-ray temperatures naturally, but would also require a standard disk to co-exist with the hotter flow to provide the optical/UV photon field and the reprocessing medium (e.g. Lasota et al. 1996; Gammie, Narayan & Blandford 1999). A serious problem for ADAFs is that the variability timescale is expected to be longer than that observed. For reasonable black hole masses of $10^{7-8} M_{\odot}$, the sound-crossing time is of order 10-100ks (Ptak et al. 1998). N98 observed large-amplitude changes on time scales at the lower end of this range, making an ADAF unlikely. It has also been suggested that flaring regions heated by magnetic reconnection might be the source of the X-ray scattering plasma (e.g. Nayakshin & Melia, 1997; Poutanen & Fabian 1999). Such regions might be highly chaotic and unstable, and could produce rapid intrinsic variability. We hope our new results will encourage a more quantitative comparison of these models with the available data.

6.5. Comparison with other campaigns

There has been some discussion (e.g. N98; Edelson et al. 2000) about the apparent discrepancies between multi-waveband variability campaigns for Seyfert galaxies. Some have found significant correlations (e.g. Clavel et al. 1992; Edelson et al. 1996), while others have apparently shown weak, complex or null relations (e.g. Done et al. 1990; Marshall et al. 1997; N98; Maoz et al. 2000; Edelson et al. 2000). Our data have shown that, before a complete picture of the multi-waveband variability can emerge, one must consider the X-ray spectral properties. Such considerations could easily account for the apparently discrepant behavior between objects, and the apparent complexities observed in individual sources. In the presence of X-ray spectral variability, the source of reprocessing photons can change between the hard and soft X-ray bands. If the reprocessing picture outlined above is correct, the interband relationships could vary in complexity, depending sensitively on the exact spectral shape in the X-rays and the ionization state of the reprocessor, both of which can be variable. Roughly speaking, we expect objects with flat X-ray spectra ($\Gamma \ll 2.0$) to show a good correlation between the hard X-ray and UV variability, as Compton downscattering dominates the heating. If the X-ray spectrum is steeper, photoelectric heating will dominate, and we then predict that the soft X-rays should correlate with the UV. Of course, if there is a high energy cutoff in the X-ray spectrum this would reduce the importance of Compton heating, as substantial ionization of the reprocessor would lead to photoelectric absorption. Presumably spectral changes due to the radiation processes could occur in the UV and optical too, making it all the more dangerous to make inferences from narrow-band observations.

To take some specific examples, we note that in NGC 4151 (Edelson et al. 1996), the best-sampled multi-wavelength campaign before the current dataset was obtained, a correlation was observed between the *soft* X-rays and the UV, just as we infer here. NGC 4151 has a relatively flat X-ray spectrum (Yaqoob & Warwick 1991), but also exhibits a cutoff in the primary spectrum at a relatively low energy (~ 50 keV; Maisack et al. 1993; Zdziarski et al. 1996), which may reduce the importance of Compton heating.

NGC 3516 has been the subject of two major recent campaigns. The first covered long time scales, where Maoz et al. (2000) showed a poor zero-lag correlation between the X-ray and optical, with no clear relationship at any lag. There was possible evidence for the optical leading the X-ray by ~ 100 d in the early part of the observation, but this broke down in the later stages. The Maoz et al. data could be explained by X-ray spectral variability, which is clearly observed in NGC 3516 on long time scales. For example, Nandra et al. (1999) noted a spectral index $\Gamma = 1.5$ in a 1997 *ASCA* observation, which can be compared to $\Gamma = 1.9$ for observations made in 1994-1995 (Nandra et al. 1997). The campaign of

Edelson et al. (2000) covered only a ~ 3 d period but was sampled very intensively with *RXTE* and *HST*. The X-ray data showed variations much larger in amplitude than those in the optical, which can be accounted for by the light-travel smoothing we suggest for NGC 7469. On the other hand the optical did show small but significant rapid variations, which showed no obvious relation to the 2-10 keV X-ray variations. The amplitude of those variations was extremely small, however, so they could merely represent variations (intrinsic or via reprocessing) in the innermost part of the disk. In the case of both long and short-term variations, an examination of the *RXTE* spectral data for NGC 3516 could be most revealing.

In NGC 5548, Clavel et al. (1992) noted a correlation between the 2-10 keV X-rays and the UV, albeit with few points and poor sampling. Marshall et al. (1997) showed that the EUV and UV variations were also well correlated, consistent with photoelectric reprocessing being a dominant effect. Completing the picture, Chiang et al. (2000) show that the EUV variations are well correlated with those in the 2-10 keV band. These workers also show a correlation between Γ and the 2-10 keV flux, and therefore presumably with the EUV/UV fluxes as well. This behavior is entirely consistent with what we observe in NGC 7469, and our model for that behavior.

We are grateful to the *RXTE* GOF and PCA instrument teams for their help and support in the data analysis. KN is supported by NASA grant NAG5-7067 to the Universities Space Research Association. BMP acknowledges support by NASA LTSA grant NAG5-8397 to Ohio State University.

A. The apparent correlation between Γ and A_{ref}

As stated in the main text, parameters derived in a single spectral fit can be correlated due to the presence of statistical errors. This is of particular concern in the case of the correlation between Γ and A_{ref} , which are highly correlated in the spectral fits. To illustrate this further we plot in Fig. 7 confidence contours of the two parameters for three of the spectra, which are elongated in the direction of the correlation.

We have performed simulations to verify whether the observed correlation between Γ and A_{ref} is an artifact of the analysis. First, we constructed 30 simulated spectra (i.e the number of daily segments) with Γ and A_{ref} covering the observed ranges ($\Gamma = 1.7 - 2.0$ and $A_{\text{ref}} = 0.002 - 0.010$). The count rate was set at the mean value ($\sim 10 \text{ ct s}^{-1}$) and the exposure time at the mean for the daily segments. The 30 simulated spectra were then fit with the same model as the real data and the correlation coefficient calculated. We

repeated this 100 times. The mean linear correlation coefficient was found to be $r = 0.12$ with a standard deviation of 0.10. The maximum value obtained was 0.32. These can be compared with the value derived from our data of $r = 0.75$. Very similar results were obtained for the rank correlation coefficient. This shows that purely statistical effects are highly unlikely to reproduce the observed correlation.

The spectral fits in Table 1 are made under the assumption that the observed power law slope is the same as that which illuminates the material responsible for the Compton reflection. In our case, as Γ is variable, so is the shape of the reflection component. If, in fact, the shape (and flux) of the Compton reflection is constant, then our fitting could result in an apparently-variable A_{ref} , which is correlated with Γ . Physically, this might be expected in a case where the reflecting material had a large physical extend, in which case the medium would respond to the “mean” Γ rather than the instantaneous value obtained in one of our one day snapshots. Simulations confirm that this can produce an apparent correlation between the parameters. If we make artificial spectra with a constant reflection component with illuminating $\Gamma = 1.92$ (the mean value), then we find a clear correlation between Γ and A_{ref} when fitting with variable- Γ model. Typical correlation coefficients are $r \sim 0.7$, similar to that observed.

An analogous situation is when there are systematic errors in the background subtraction - particularly a systematic underestimate. These can also cause an apparent correlation between the parameters. We have simulated such an effect by making simulated spectra with the parameters actually derived from the individual daily segments, but before fitting, artificially modifying the background spectrum so that it underestimates the flux at high energies. In particular we changed the PCA background spectrum such that the error had a roughly power-law form, which rose from zero at low energies to a maximum value of ~ 3 per cent at 20 keV. This represents a ~ 30 per cent error in the source-minus-background spectrum at these energies. Repeating the 30-spectrum simulation 100 times, we obtained correlation coefficients in the range 0.7-0.8, again similar to the observed value of 0.75.

We conclude that the observed (and apparently highly significant) correlation between Γ and A_{ref} observed in our spectral fits could easily be due either to a reflection component with constant shape and flux, or to a systematic under-subtraction of the background.

Table 1. Spectral fits to daily segments

Day TJD	Exposure ks	F_{2-10} 10^{-11}	Γ	$F_{K\alpha}$ 10^{-5}	A_{ref} 10^{-3}	χ^2 43 d.o.f.
245.104	18.8	3.43	1.973 ± 0.045	5.50 ± 0.96	6.4 ± 3.7	47.9
246.177	18.4	3.45	1.979 ± 0.045	4.99 ± 0.97	5.3 ± 3.6	48.5
247.247	16.1	2.89	1.929 ± 0.053	5.35 ± 1.00	2.3 ± 2.9	44.1
248.316	15.5	3.72	1.919 ± 0.043	5.32 ± 1.07	4.2 ± 3.2	65.2
249.386	14.8	3.81	1.928 ± 0.044	5.30 ± 1.10	4.0 ± 3.3	64.6
250.456	13.1	3.92	1.902 ± 0.040	4.75 ± 1.17	1.9 ± 2.6	39.8
251.579	16.5	3.40	1.832 ± 0.042	5.95 ± 1.02	2.8 ± 2.4	70.4
252.631	16.1	3.17	1.860 ± 0.047	5.59 ± 1.02	4.1 ± 2.8	43.4
253.676	15.0	2.55	1.707 ± 0.052	3.98 ± 1.00	1.2 ± 1.6	53.1
254.714	14.5	3.17	1.874 ± 0.049	5.70 ± 1.07	2.5 ± 2.8	46.7
255.777	12.5	2.81	1.909 ± 0.065	5.82 ± 1.13	5.8 ± 4.0	63.3
256.811	15.2	2.76	1.853 ± 0.057	4.90 ± 1.02	5.1 ± 3.1	49.7
257.840	13.9	2.75	1.882 ± 0.063	4.80 ± 1.07	6.5 ± 3.8	43.0
258.865	15.8	2.55	1.930 ± 0.068	4.42 ± 0.99	6.9 ± 4.3	50.8
259.914	16.6	2.87	1.980 ± 0.063	4.43 ± 0.99	10.2 ± 5.1	44.9
260.914	14.0	2.61	1.926 ± 0.069	4.83 ± 1.05	6.5 ± 4.3	51.6
261.918	15.4	2.83	1.943 ± 0.060	5.40 ± 1.02	6.2 ± 4.0	42.7
262.882	13.3	3.37	1.983 ± 0.056	4.99 ± 1.13	7.4 ± 4.8	54.2
263.883	19.6	3.29	2.009 ± 0.050	4.47 ± 0.93	10.2 ± 4.6	49.7
264.917	15.6	3.53	1.959 ± 0.045	5.26 ± 1.05	3.7 ± 3.4	41.2
265.953	18.2	3.91	1.957 ± 0.041	5.02 ± 1.00	7.8 ± 3.7	68.4
267.019	18.2	4.04	1.899 ± 0.036	6.11 ± 1.01	3.6 ± 2.7	61.2
268.084	18.4	3.93	1.939 ± 0.039	5.48 ± 1.00	6.6 ± 3.3	60.2
269.155	19.4	3.86	1.867 ± 0.032	6.51 ± 0.97	1.2 ± 1.8	66.7
270.222	16.5	3.33	1.847 ± 0.043	5.72 ± 1.01	2.9 ± 2.5	44.9
271.282	17.9	3.41	1.821 ± 0.035	5.16 ± 0.98	1.0 ± 1.6	62.8
272.361	16.5	2.72	1.774 ± 0.050	4.88 ± 0.97	2.2 ± 2.0	57.6
273.417	20.1	2.66	1.872 ± 0.053	3.24 ± 0.87	5.3 ± 3.0	59.9
274.488	19.4	3.22	1.902 ± 0.044	5.30 ± 0.93	5.3 ± 2.9	47.5
275.547	21.4	3.22	2.014 ± 0.049	4.76 ± 0.89	10.3 ± 4.5	59.9

Note. — F_{2-10} is in units of $\text{erg cm}^{-2} \text{s}^{-1}$; $F_{K\alpha}$ is in units of $\text{photon cm}^{-2} \text{s}^{-1}$. A_{ref} is defined in the text.

Table 2. Correlations between the parameters

	F_{2-10}	$F_{K\alpha}$	Γ	A_{ref}	F_{UV}	$Q_{0.1-100}$	$F_{\text{UV}extrap}$
F_{2-10}	...	<i>0.54</i>	0.21	-0.23	0.22	<i>0.73</i>	0.45
$F_{K\alpha}$	<i>0.52</i>	...	0.01	-0.34	0.02	0.25	0.04
Γ	0.13	-0.20	...	<i>0.75</i>	<i>0.81</i>	<i>0.81</i>	<i>0.92</i>
A_{ref}	-0.26	-0.36	<i>0.75</i>	...	<i>0.50</i>	0.41	<i>0.64</i>
F_{UV}	0.26	-0.05	<i>0.85</i>	<i>0.49</i>	...	<i>0.71</i>	<i>0.80</i>
$Q_{0.1-100}$	<i>0.71</i>	0.18	<i>0.75</i>	0.37	<i>0.68</i>	...	<i>0.94</i>
$F_{\text{UV}extrap}$	<i>0.47</i>	-0.02	<i>0.92</i>	<i>0.58</i>	<i>0.82</i>	<i>0.93</i>	...

Note. — The upper right portion of the table shows the Pearson linear correlation coefficient. The lower left part shows the Spearman (rank) correlation coefficients. The correlations have 30 points, except for those with F_{UV} which have 29. Approximately, values of $|r| > 0.36, 0.46, 0.57$ are formally significant at $> 95, 99, 99.9$ per cent confidence. Those correlation coefficients with formal chance probabilities < 1 per cent are shown in italics, although we note that these probabilities can be modified when dealing with “red noise” light curves (see text).

REFERENCES

- Blandford, R.D., McKee, C.F., 1982, *ApJ*, 255, 419
- Brandt, W.N., Fabian, A.C., Nandra, K., Tsuruta, S., 1993, *MNRAS*, 265, 996
- Chen, K., Halpern, J.P., Filippenko, A., 1989, *ApJ*, 339, 742
- Chiang, J., et al., 2000, *ApJ*, 528, 292
- Clavel, J., et al., 1991, *ApJ*, 366, 64
- Clavel, J., et al., 1992, *ApJ*, 393, 113
- Collier, S., et al. 1998, 500, 162
- Courvoisier, T., J.-L., Clavel, J., 1991, *A&A*, 248, 389
- De Rosa, A., et al., 2000, “X-ray Astronomy 1999”, in press
- Done, C., Ward, M.J., Fabian, A.C., Kunieda, H., Tsuruta, S., Lawrence, A., Smith, M.G., Wamsteker, W., 1990, *MNRAS*, 243, 713
- Edelson, R.A., et al., 1996, *ApJ*, 470, 364
- Edelson, R.A., et al., 2000, *ApJ*, in press
- Elvis, M., Lockman, F.J., Wilkes, B.J., 1989, *AJ*, 97, 777
- Eracleous, M., Halpern, J.P., 1994, *ApJS*, 90, 1
- Fabian, A.C., Nandra, K., Reynolds, C.S., Brandt, W.N., Otani, C., Tanaka, Y., Inoue, H., Iwasawa, K., 1995, *MNRAS*, 277, L11
- Gammie, C.F., Narayan, R., Blandford, R., 1999; *ApJ*, 516, 177
- Gaskell, C.M., Peterson, B.M., 1987, *ApJS*, 65, 1
- Genzel, R., Weitzel, L., Tacconi-Garman, L.E., Blietz, M., Cameron, M., Krabbe, A., Lutz, D., Sternberg, A., 1995, *ApJ*, 444, 129
- George, I.M., Fabian, A.C., 1991, *MNRAS*, 249, 352
- Ghisellini, G., George, I.M., Fabian, A.C., Done, C., *MNRAS*, 248, 14
- Ghisellini, G., Haardt, F., Matt, G., 1994, *MNRAS*, 267, 743
- Gondek, D., et al., 1996, *MNRAS*, 282, 646
- Green, A.R., McHardy, I.M., Lehto, H.J., 1993, *MNRAS*, 265, 664
- Guainazzi, M., Matsuoka, M., Piro, L., Mihara, T., Yamauchi, M., 1994, *ApJ*, 436, L35
- Guilbert, P.W., Rees, M.J., 1988, *MNRAS*, 233, 475
- Haardt, F., Maraschi, L., 1991, *ApJ*, 380, 51

- Haardt, F., Maraschi, L., 1993, *ApJ*, 413, 507
- Haardt, F., Maraschi, L., Ghisellini, 1994, *ApJ*, 432, L95
- Holt, S.S., Mushotzky, R.F., Boldt, E.A., Serlemitsos, P.J., Becker, R.H., Szymkowiak, A.E., White, N.E., 1980, *ApJ*, 241, L13
- Iwasawa, K., et al., 1996, *MNRAS*, 282, 1038
- Iwasawa, K., Fabian, A.C., Young, A.J., Inoue, H., Matsumoto, C., 1999, *MNRAS*, 306, L19
- Krolik, J.H., Horne, K., Kallman, T.R., Malkan, M.A., Edelson, R.A., Kriss, G.A., 1991, *ApJ*, 371, 541
- Kriss, G.A., Peterson, B.M., Crenshaw, D.M., Zheng, Wei, 2000, *ApJ*, in press
- Krolik, J.H., Madau, P., Zycki, P.T., 1994, *ApJ*, 420, L57
- Lasota, J.-P., Abramowicz, M., Chen, X., Krolik, J., Narayan, R., Yi, I. 1996, *ApJ*, 462, L142
- Leighly, K., Mushotzky, R.F., Yaqoob, T., Kunieda, H., Edelson, R.A., 1996, *ApJ*, 469, 147
- Lynden-Bell, D., 1969, *Nature*, 223, 690
- Madejski, G.M., et al., 1995, *ApJ*, 438, 672
- Magdziarz, P., Zdziarski, A.A., 1995, *MNRAS*, 273, 837
- Maisack, M., et al., 1993, *ApJ*, 407, L61
- Malkan, M.A., Sargent, W.L., 1982, *ApJ*, 254, 22
- Maoz, D., Edelson, R.A., Nandra, K., *AJ*, 119, 119
- Matsuoka, M., Piro, L., Yamauchi, M., Murakami, T., 1990, *ApJ*, 361, 440
- Matt, G., in “X-ray Astronomy 1999”, in press
- Matt, G., Perola, G.C., Piro, L., 1991, *A&A*, 245, 63
- Miyoshi, S., 1995, *Nature*, 373, 127
- Molendi, S., Maraschi, L., Stella, L., 1992, *MNRAS*, 255, 27
- Nandra, K., et al., 1998, *ApJ*, 505, 594 (N98)
- Nandra, K., George, I.M., Mushotzky, R.F., Turner, T.J., Yaqoob, T., 1997, *ApJ*, 477, 602
- Nandra, K., George, I.M., Mushotzky, R.F., Turner, T.J., Yaqoob, T., 1999, *ApJ*, 523, L17
- Nandra, K., Pounds, K.A., 1994, *MNRAS*, 268, 405
- Narayan, R., Yi, I., 1994, *ApJ*, 428, L13

- Nayakshin, S., Melia, F., 1997, *ApJ*, 490, L13
- Peterson, B.M., 1993, *PASP*, 105, 247
- Peterson, B.M., et al., 1991, *ApJ*, 368, 119
- Peterson, B.M., Wanders, I., Horne, K., Collier, S., Alexander, T., Kaspi, S., Maoz, D., 1998, *PASP*, 110, 660
- Piro, L., Yamauchi, M., Matsuoka, M., 1990, *ApJ*, 360, L35
- Poutanen, J., Fabian, A.C., 1999, *MNRAS*, 306, L31
- Ptak, A., Yaqoob, T., Mushotzky, R.F., Serlemitsos, P.J., Griffiths, R.E., 1998, *ApJ*, 501, L37
- Shapiro, S.L., Lightman, A.P., Eardley, D.M., 1976, *ApJ*, 204, 187
- Shields, G.A., 1978, *Nature*, 272, 706
- Stern, B.E., Poutanen, J., Svensson, R., Sikora, M., Begelman, M.C., 1995, *ApJ*, 449, L13
- Sunyaev, R.A., Titarchuk, L.G., 1980, *A&A*, 86, 121
- Tanaka, Y., et al., 1995, *Nature*, 375, 659
- Turner, T.J., 1987, *MNRAS*, 226, 9P
- Uttley, P., McHardy, I.M., Papadakis, I.E., Cagnoni, I., Fruscione, A., 2000, *MNRAS*, in press
- Wanders, I., et al., 1997, *ApJS*, 113, 69
- Welsh, W.F., Peterson, B.M., Koratkar, A.P., Korista, K.T., 1998, *ApJ*, 509, 118
- Welsh, W.F., 1999, *PASP*, 111, 1347
- White, R.J., Peterson, B.M., 1994, *PASP*, 106, 879
- Yaqoob, T., Warwick, R.S., 1991, *MNRAS*, 248, 773
- Zdziarski, A.A., et al., 1994, *MNRAS*, 269, L55
- Zdziarski, A.A., Johnson, W.N., Magdziarz, P., 1996, *MNRAS*, 283, 193
- Zdziarski, A.A., Lubinski, P., Smith, D.A., *MNRAS*, 303, L11

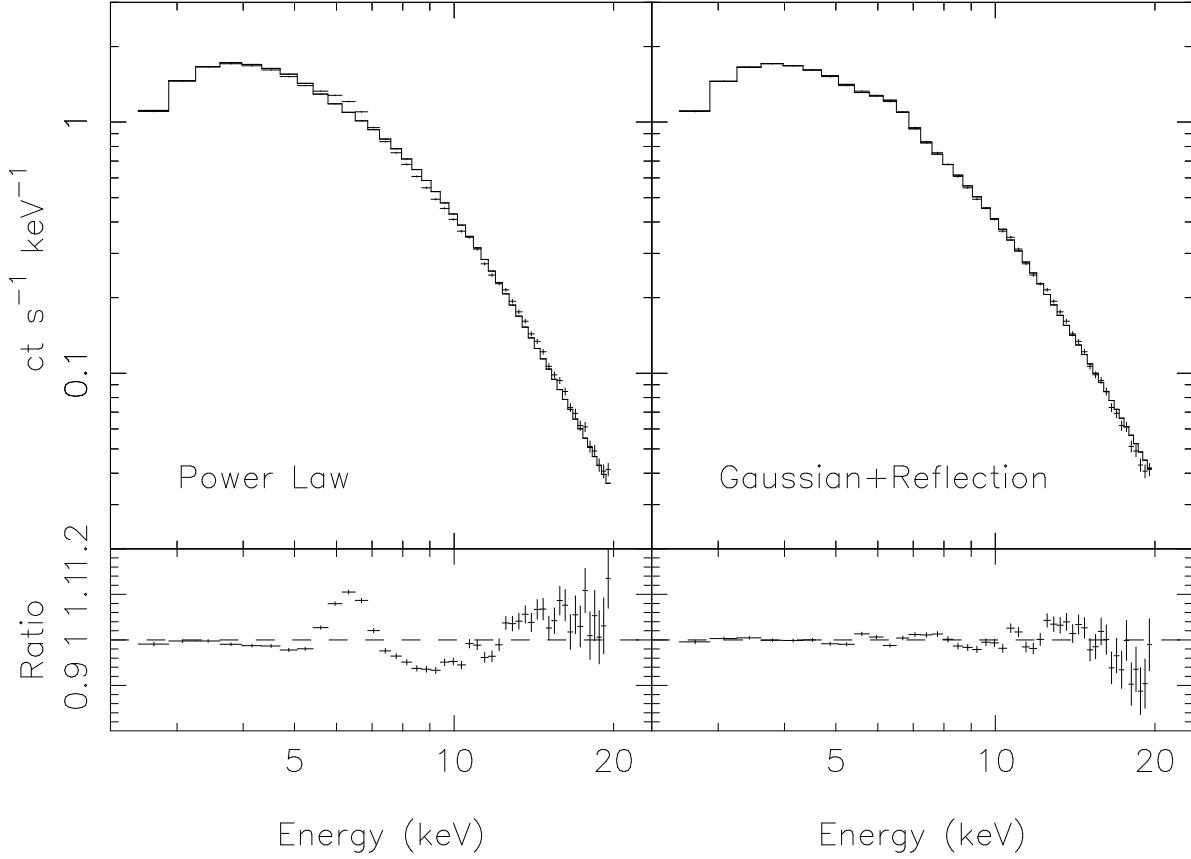


Fig. 1.— The left panels show a fit to the integrated spectrum with a power law model. The upper panel shows the counts spectrum (crosses) and model (line), after folding through the instrumental response. The lower panel shows the ratio of this model to the data, clearly demonstrating the presence of the iron $K\alpha$ line and reflection component. The fit is extremely poor, with a reduced χ^2 of $\chi^2_{\nu} = 47.6/44$ d.o.f. The right panels show the fit when a gaussian line and reflection component are introduced into the model. Though still not formally acceptable, perhaps due to systematic effects, or the fact that the spectrum is variable (see Fig. 2), it is a vast improvement, with $\chi^2_{\nu} = 3.5$ for 41 d.o.f.

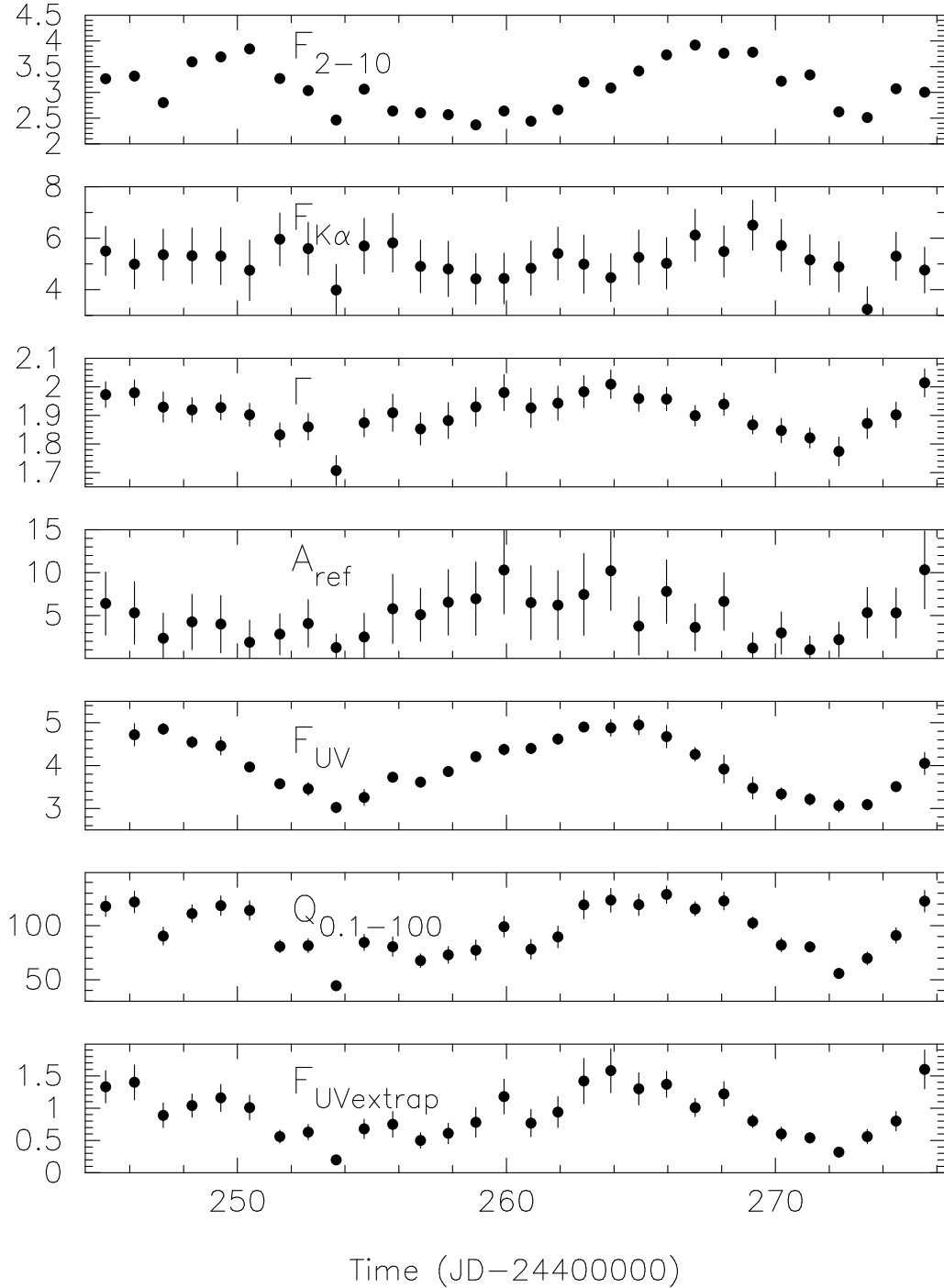


Fig. 2.— Light curves of (descending), the 2-10 keV flux (F_{2-10}), the photon index (Γ), the iron line flux ($F_{K\alpha}$), the reflection flux (A_{ref}), the UV continuum flux at 1315Å (F_{UV}), the broad-band X-ray photon flux ($Q_{0.1-100}$) and the X-ray power law flux extrapolated back to 1315Å (F_{UVextrap}). The continuum index and reflection flux are variable and not obviously related to the X-ray flux. The iron line is formally consistent with a constant but may be correlated with F_{2-10} . The light curves for Γ , A_{ref} , F_{UV} , $Q_{0.1-100}$ and F_{UVextrap} all have similar shapes and appear to be correlated with each other. See Figs. 3-5, Table 2 and the text for further details.

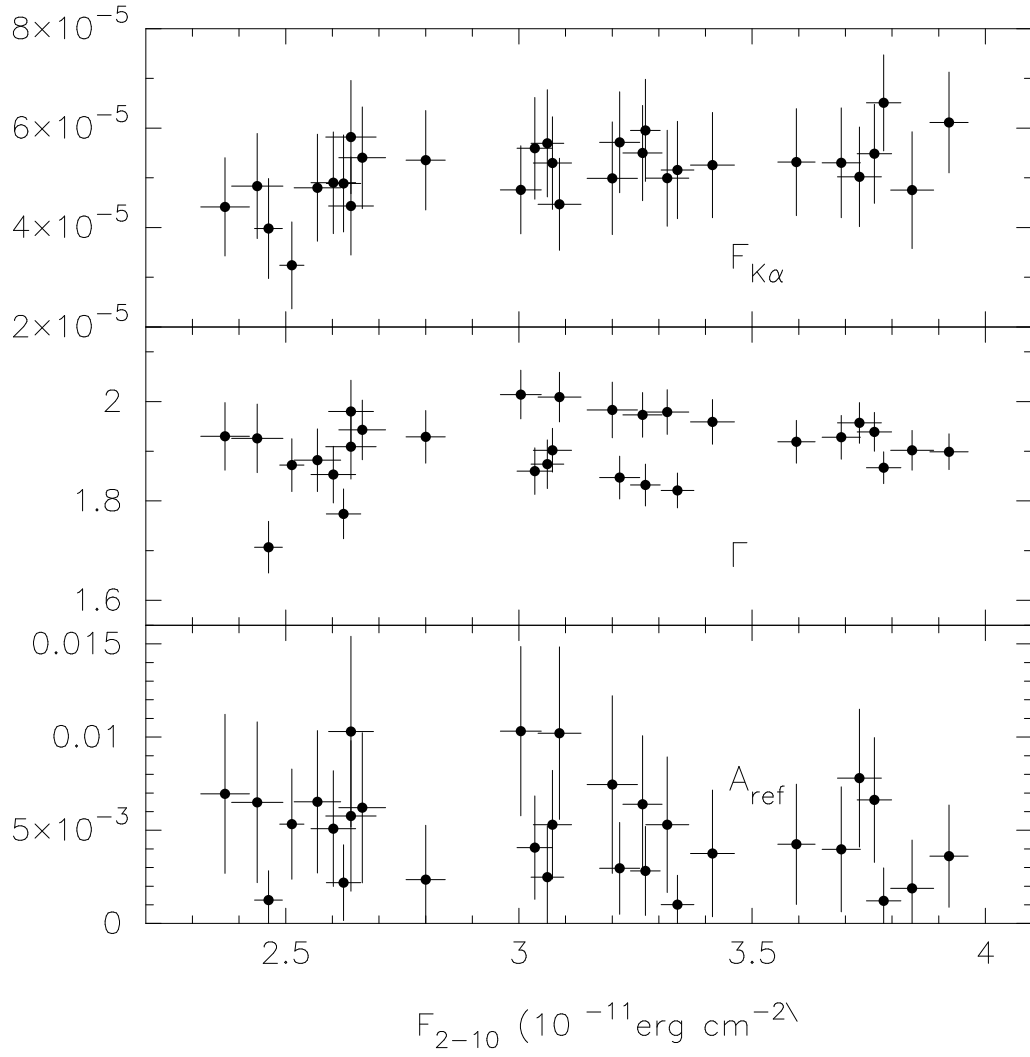


Fig. 3.— Correlations between F_{2-10} and a) line normalization $F_{K\alpha}$, b) photon index Γ and c) reflection normalization, A_{ref} . The only parameter which shows a significant correlation is the line normalization, at ~ 99.8 per cent confidence (Table 2).

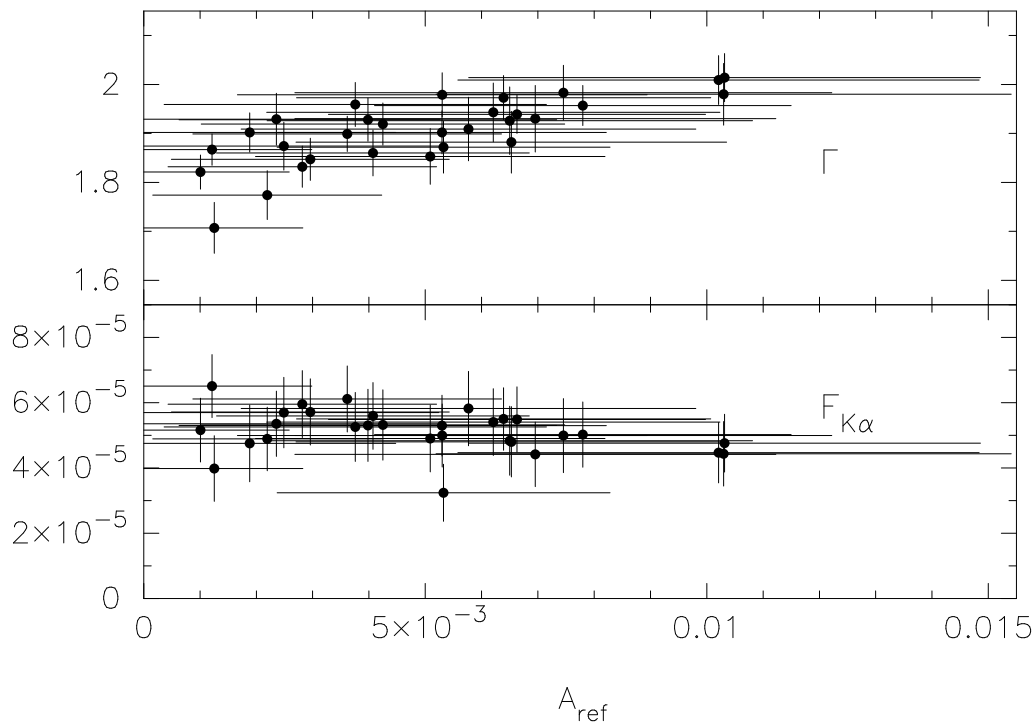


Fig. 4.— A_{ref} plotted against Γ (upper panel) and $F_{K\alpha}$ (lower panel). The former clearly shows a correlation, although much of this could be statistical in nature, due to the natural correlation between the parameters in the spectral fits (Appendix A). The latter shows no significant relationship, even though the components are thought to have a common origin as reflection from the accretion disk. The apparent variability in the reflection continuum may be due to a combination of statistical and systematic effects, however, accounting for this decoupling.

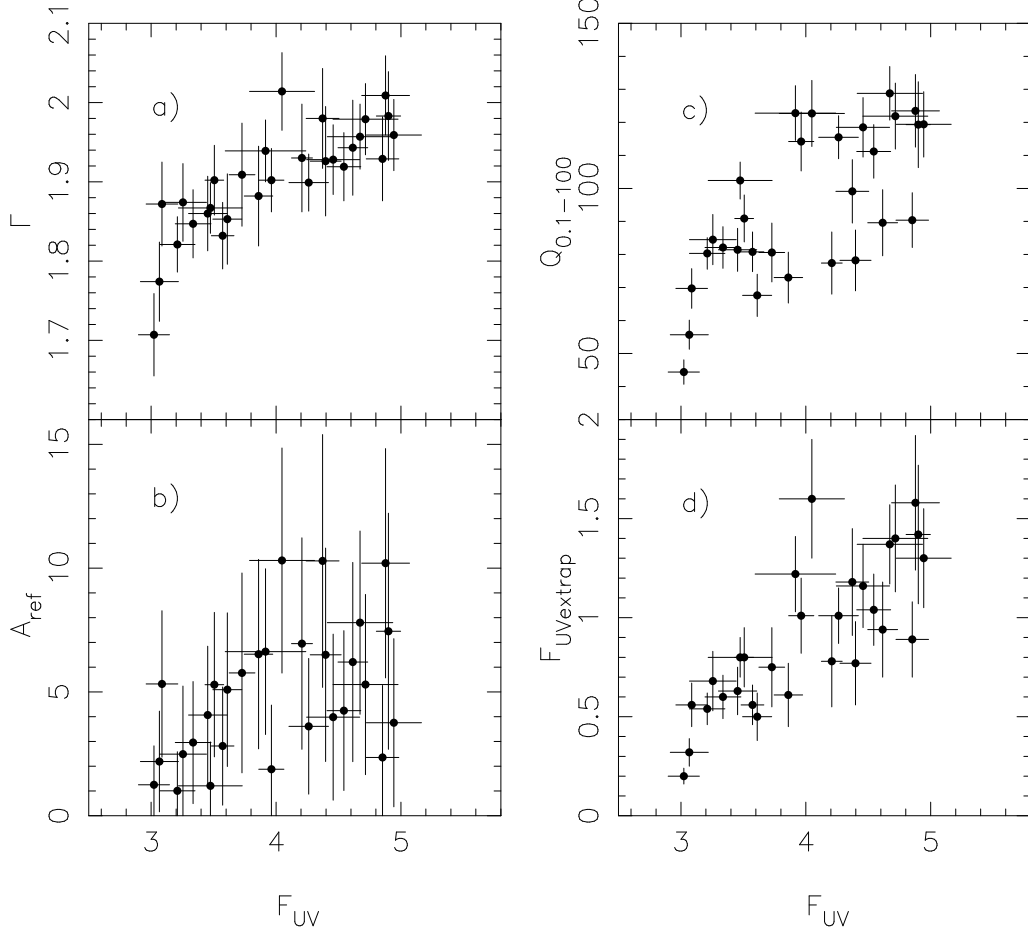


Fig. 5.— Correlations between the UV continuum flux at 1315 Å, F_{UV} and a) the photon index Γ , b) the reflection normalization, A_{ref} c) the broad-band X-ray *photon* flux, $Q_{0.1-100}$ and d) the predicted UV continuum flux at 1315 Å based on an extrapolation of the X-ray power law, $F_{UVextrap}$. The correlation with A_{ref} is rather marginal and may be exaggerated by the effect that A_{ref} and Γ are correlated, which may be spurious (Appendix A). The other correlations formally have very small chance probabilities (> 99.9 per cent confidence). The correlations of F_{UV} with Γ and photon flux strongly support the hypothesis that the X-ray flux arises from Compton upscattering of UV seed photons (see text). The final correlation illustrates the more radical hypothesis that the variable part of the UV flux may simply be an extrapolation of the X-ray power law variability. Correlation coefficients are shown in Table 2.

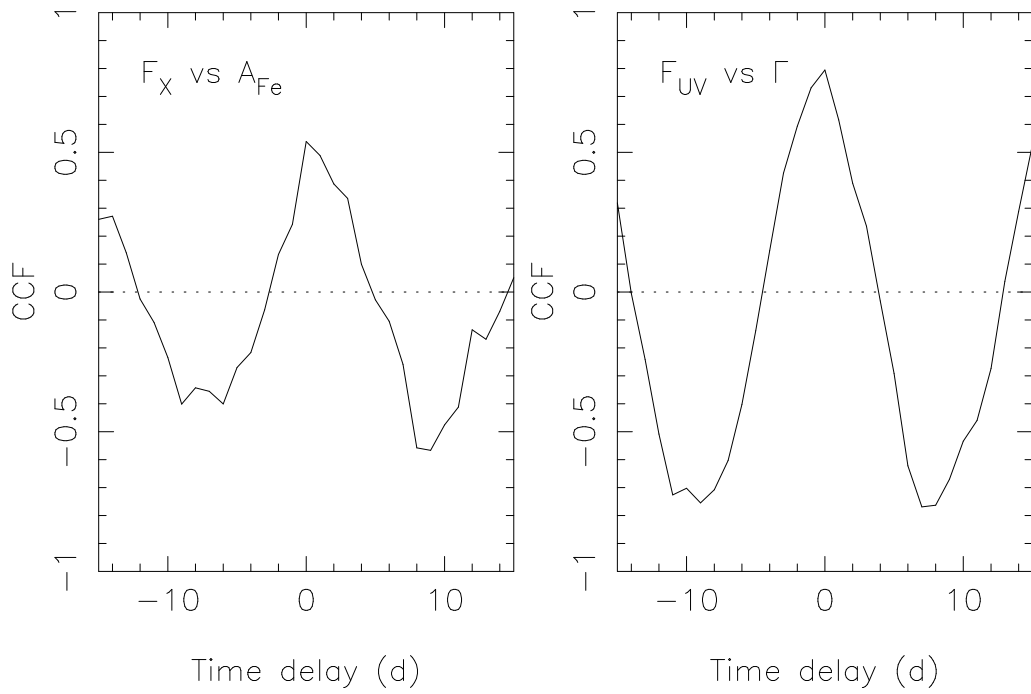


Fig. 6.— Cross-correlation function for $F_{K\alpha}$ versus F_{2-10} (left panel) and Γ versus F_{UV} (right panel). Both show a strong peak at zero lag but the data quality and sampling are not adequate to provide meaningful constraints or upper limits on the time lag.

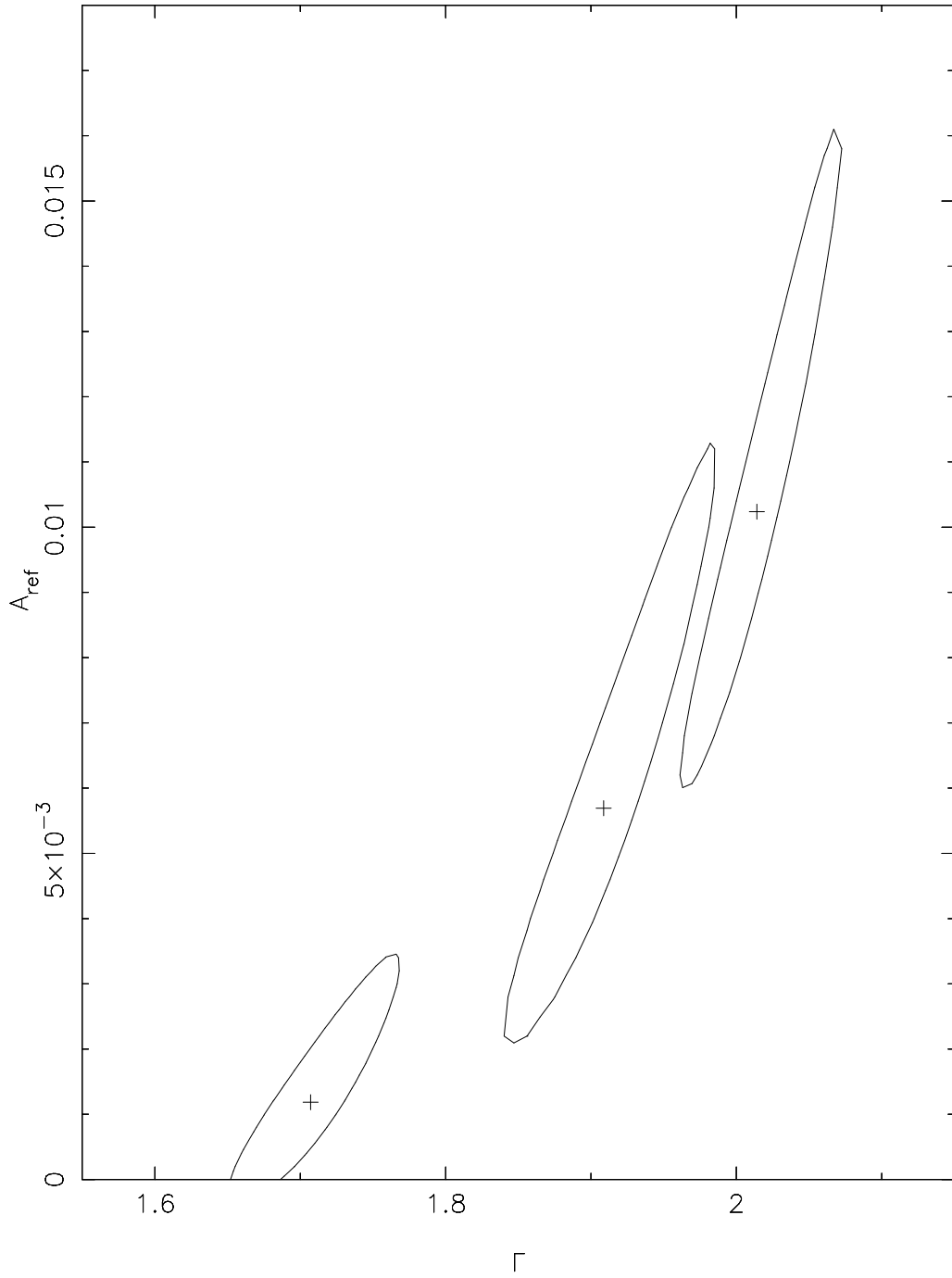


Fig. 7.— 90 per cent confidence contours for Γ and A_{ref} for the spectra of segments 9, 11 and 30, which cover the range of these parameters. The two parameters are highly correlated in the individual fits and this, combined with possible systematic effects, can cause the apparent correlation observed between the parameters seen in Fig. 4 (Appendix A)

1-Mar-2000 20:23